Nonstoichiometric Tungsten Oxide Based on Hexagonal WO 3

ARTICLE *in* CRYSTAL GROWTH & DESIGN · NOVEMBER 2001

Impact Factor: 4.89 · DOI: 10.1021/cg015545z

CRYSTAL GROWTH & DESIGN
2001
VOL. 1, NO. 6
473−477

Nonstoichiometric Tungsten Oxide Based on Hexagonal WO_3

Yu. M. Solonin,* O. Yu. Khyzhun, and E. A. Graivoronskaya

Institute for Problems of Materials Science, National Academy of Sciences of Ukraine, 3 Krzhyzhanovsky str., UA-03142 Kyiv, Ukraine

Received August 2, 2001

ABSTRACT: On the initial stage of reduction of hexagonal tungsten trioxide, h-WO_3, the nonstoichiometric h-$WO_{2.8}$ phase was synthesized. The X-ray powder diffraction analysis and subsequent refinement using the Rietveld Full Profile Matching & Integrated Intensities Refinement of X-ray and/or Neutron Data Programs (FullProf Version 3.5 Dec97-LLB-JRC) indicate that the crystal structure of the h-$WO_{2.8}$ phase is ascribed to the UO_3 structure type with lattice parameters $a = 0.3625$ nm and $c = 0.3780$ nm. The X-ray photoelectron spectroscopy (XPS) method was applied to study the electronic structure of the nonstoichiometric tungsten trioxide. The XPS valence band and core-level spectra of the h-$WO_{2.8}$ phase and, for comparison, h-WO_3 were derived. The formation of an additional near-Fermi subband, which is absent on the XPS valence-band spectrum of hexagonal tungsten trioxide, was observed on the spectrum of the nonstoichiometric hexagonal $WO_{2.8}$ compound. Half-widths of the XPS valence band as well as both W 4f and O 1s core-level spectra increase somewhat when going from h-WO_3 to h-$WO_{2.8}$.

1. Introduction

Reduction of monoclinic tungsten trioxide, m-WO_3, leads to formation of the so-called Magnéli phases[1] belonging to the homologous series W_nO_{3n-1} and W_nO_{3n-2}, having ordered {102} and {103} crystallographic shear (CS) planes, respectively.[2−4] The Magnéli phases consist of largely unchanged slabs of tungsten trioxide joined along the mentioned CS planes. The crystal structure of pure m-WO_3 belongs to the pseudocubic ReO_3 type; i.e., it can be represented as constructed from [W−O_6] octahedra linked by corner sharing, and their arrangement results in a simple cubic symmetry (Figure 1). Nevertheless, the structure is less symmetrical then ReO_3 because of distortions of the [W−O_6] octahedra.[5] In addition to low-temperature m-WO_3 reduction, the Magnéli phases may be also prepared under equilibrium conditions from the corresponding components.

The new hexagonal form of tungsten trioxide, h-WO_3, has been synthesized comparatively recently by Gerand et al.[6] by dehydration due to dry heating of the hydrate $WO_3 \cdot {}^1/_3H_2O$. Since then, h-WO_3 has been intensively investigated, especially as an intercalation host for obtaining hexagonal tungsten bronzes M_xWO_3 and a promising material for positive electrodes of rechargeable lithium batteries. A number of alternative methods for synthesis of h-WO_3 were proposed (a review of the synthetic routes for obtaining the hexagonal form of tungsten trioxide has been made recently by Han et al.[7]). The structure of h-WO_3 is presented in Figure 2. As can be seen from the figure, the corner-sharing [W−O_6] octahedra form hexagonal channels oriented along the *c* axis. According to the results of Gerand et al.,[6] the structure of h-WO_3 is described in the space group $P6/mmm$ with cell parameters $a = 0.7298$ nm and $c = 0.7798$ nm.

Previously, one of the present authors and others[8] proposed to prepare h-WO_3 using the low-temperature selective reduction of copper tungstate, $CuWO_4$, with subsequent Cu separation by dissolving in HNO_3. During the investigation of this process, the hexagonal hydrogen tungsten bronze $H_{0.24}WO_3$ was observed as an intermediate phase.[8] The oxidation of $H_{0.24}WO_3$ in air resulted in formation of h-WO_3 with cell parameters $a = 0.7276$ nm and $c = 0.7800$ nm, which are close to those obtained by Gerand et al.[6] The above $H_{0.24}WO_3$ and h-WO_3 compounds were studied very recently in refs 9 and 10 using the X-ray photoelectron (XPS), emission (XES), and absorption (XAS) spectroscopy methods.

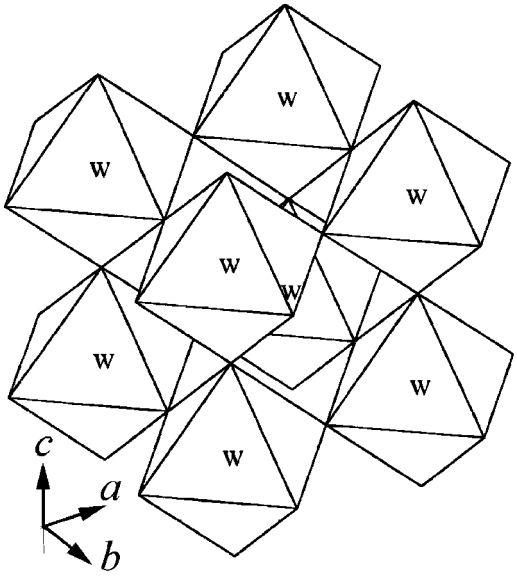

Figure 1. Arrangement of [W−O_6] octahedra in the structure of monoclinic WO_3.

In the present paper we report the results of a study concerning phase transformation at low-temperature reduction of h-WO_3 by hydrogen. We paid special attention to the earliest reduction stage when the appearance of nonstoichiometric phases similar to the Magnéli phases might be expected. Peculiarities of the atomic and electronic structures of the nonstoichiomet-

10.1021/cg015545z CCC: $20.00
Published on Web 10/19/2001

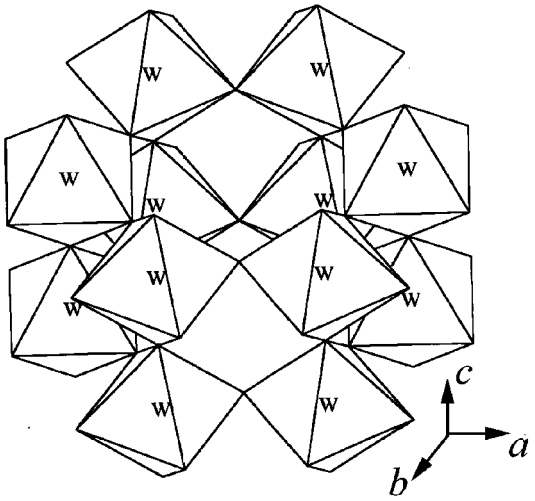

Figure 2. Arrangement of [W−O_6] octahedra in the structure of hexagonal WO_3.

ric phase based on h-WO_3 were studied as well. It should be mentioned that, while the electronic structure of nonstoichiometric compounds WO_x belonging to the monoclinic symmetry group was studied in a series of experimental works,[3,11,12] to our knowledge, the electronic structure of nonstoichiometric tungsten trioxides belonging to the hexagonal symmetry group has not been investigated by either experimental or theoretical methods. The band structure of stoichiometric h-WO_3 was calculated using a self-consistent and relativistic version of a full-potential linear muffin-tin orbital (FP-LMTO) method by Hjelm et al.[13]

2. Experimental Section

Copper tungstate, $CuWO_4$, was used as a precursor for obtaining both the stoichiometric and nonstoichiometric hexagonal tungsten trioxides studied in the present work. The precursor was obtained by a solid-state reaction of CuO and the usual monoclinic form of tungsten trioxide, m-WO_3, according to the relation $CuO + WO_3 = CuWO_4$.[8,14] The solid-state reaction was carried out in air at 800 °C. The reduction of $CuWO_4$ was performed in hydrogen at 300 °C. A product of the reduction was treated by concentrated HNO_3 up to the full desolving of copper. After washing and drying, a precipitate was found to be the hexagonal phase of hydrogen tungsten bronze, H_xWO_3, with $x = 0.24$.[15] The oxidation of $H_{0.24}WO_3$ in air at 400−450 °C was used to obtain pure h-WO_3. The reduction of h-WO_3 was carried out in hydrogen at 450−500 °C. We utilized a through passage reactor and dried hydrogen; the technique was analogous to that described elsewhere.[8,16] The content of intermediate phases was evaluated using the weight analysis method.[16] Conventional X-ray diffraction analysis was used to determine the lattice parameters of the phases obtained. The X-ray analysis was done with a DRON-3 diffractometer using Cu Kα radiation. A more detailed study of the crystal structure of nonstoichiometric hexagonal tungsten trioxide, h-WO_{3-x}, was made using the Rietveld Full Profile Matching & Integrated Intensities Refinement of X-ray and/or Neutron Data Programs (FullProf Version 3.5 Dec97-LLB-JRC).

Measurements of the XPS valence-band and core-level spectra of the h-WO_3 and h-WO_{3-x} samples were carried out in an ion-pumped chamber of an ES-2401 spectrometer. The chamber was evacuated to 2×10^{-7} Pa. The Mg Kα ($E = 1253.6$ eV) excitation was used as the source of X-ray radiation. The impurity carbon 1s line (285.0 eV) was taken as the reference.

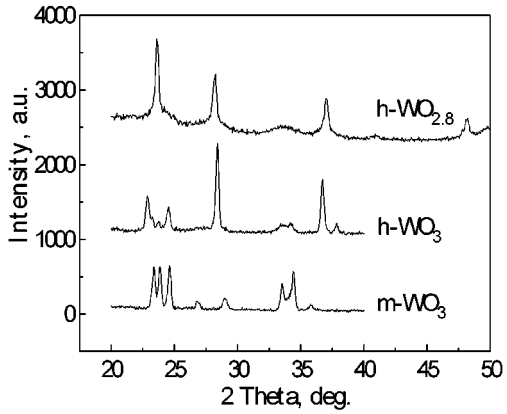

Figure 3. X-ray powder diffraction patterns of monoclinic WO_3 and hexagonal WO_3 and $WO_{2.8}$.

3. Results and Discussion

3.1. Crystal Structure. Figure 3 shows excerpts of X-ray diffraction patterns of m-WO_3 used as an initial product, the intermediate h-WO_3 phase, and the nonstoichiometric WO_{3-x} phase derived due to hydrogen reduction of h-WO_3. The h-WO_3 phase was derived from copper tungstate, $CuWO_4$, with subsequent copper dissolution in HNO_3 and following oxidation of the $H_{0.24}$-WO_3 phase, as mentioned in the Experimental Section (for detailed information see refs 8 and 14). As can be seen from Figure 3, the studied h-WO_3 specimen was mainly a single-phase material and contained small amounts of m-WO_3.

Hydrogen reduction of h-WO_3 at 450 °C leads to formation of an earlier unknown nonstoichiometric phase of tungsten oxide (Figure 3). The X-ray diffraction pattern of the phase contains also small diffusive lines of partly reduced nonstoichiometric tungsten trioxide. Positions of the lines correspond to monoclinic $WO_{2.9}$ (the well-known $W_{20}O_{58}$ Magneli phase[1]). In the following analysis of the crystal structure of the new phase, these diffusive lines will not be taken into account.

The weight analysis has shown that the relative content of the oxygen atoms in the nonstoichiometric phase obtained from h-WO_3 corresponds to the formula of $WO_{2.8}$. More detailed X-ray diffraction analysis data for the $WO_{2.8}$ phase are listed in Table 1 as sets of both experimentally derived and theoretically calculated interlayer d_{hkl} distances, which are compared with analogous data for h-WO_3. The h-WO_3 phase possesses the lattice parameters $a = 0.7276$ nm and $c = 0.3900$ mn.[8] Our results differ from those of ref 6 by a doublet value of the c parameter. Gerand et al.[6] observed a number of additional small reflexes. The interpretation of the reflexes demanded the doubling of the c parameter. We did not observe such reflexes in our experiments.

As one can see from data listed in Table 1, the unknown $WO_{2.8}$ phase can be described in a hexagonal lattice. It is observed also that the X-ray diffraction data for $WO_{2.8}$ can be derived from those of h-WO_3 by retaining the reflexes with odd values of h and k. Therefore, similar to h-WO_3, for the $WO_{2.8}$ phase all the d_{hkl} values are described using a hexagonal primitive cell, provided $a(WO_{2.8}) \approx {}^1/_2[a(\text{h-}WO_3)]$. The observed similarity of X-ray diffraction data for the h-WO_3 and

Table 1. X-ray Diffraction Data for h-WO_3 and h-$WO_{2.8}$

h-WO_3: a = 0.7276 nm; c = 0.3900 nm			h-$WO_{2.8}$: a = 0.3625 nm; c = 0.3780 nm		
hkl	*d*(obsd)	*d*(calcd)	*hkl*	*d*(obsd)	*d*(calcd)
100	0.6300	0.6301			
001	0.3894	0.3900	001	0.3780	0.3780
110	0.3631	0.3638			
200	0.3151	0.3151	100	0.3142	0.3139
201	0.2451	0.2451	101	0.2412	0.2415
210	0.2380	0.2382			
300	0.2098	0.2100			
002	0.1950	0.1950	002	0.1890	0.1890
220	0.1819	0.1819	110	0.1812	0.1813
310	0.1747	0.1748			
202	0.1656	0.1658	111	0.1634	0.1634
221	0.1650	0.1649	102	0.1617	0.1619
311	0.1595	0.1595			
400	0.1576	0.1575			
401	0.1461	0.1461	201	0.1454	0.1450
			112	0.1307	0.1308
			003	0.1260	0.1260
			202	0.1208	0.1208
			103	0.1169	0.1169
			301	0.1004	0.1004
			203	0.9820	0.9820
			004	0.9460	0.9460
			104	0.9050	0.9050
			114	0.8380	0.8380

$WO_{2.8}$ phases indicates that the partial reduction of h-WO_3 leads to formation of a nonstoichiometry on the oxygen sublattice phase of tungsten oxide; the initial motif of the hexagonal structure remains constant. Despite all this, the structure of the forming nonstoichiometric phase is more symmetric than that of the initial h-WO_3 phase.

A comparison of the X-ray diffraction data (Table 1) for the studied nonstoichiometric hexagonal tungsten oxide, h-$WO_{2.8}$, with that for pseudohexagonal Nb_2O_5[17] shows that a close similarity of the d_{hkl} sets for these phases is observed. The authors of ref 17 consider that the structure of h-Nb_2O_5 is based on a cation sublattice similar to that of UO_3. The structure of UO_3 represents a simple hexagonal unit cell and is built from alternating hexagonal layers of uranium and oxygen atoms.[18] Arrangements of the W and U atoms in hexagonal layers of h-WO_3 and UO_3 are shown in parts a and c, respectively, of Figure 4. The tungsten atoms belonging to the (001) plane of h-WO_3 occupy nodes of the hexagonal lattice similar to those of the U atoms in the (001) plane of UO_3, except that of the fourth part of the nodes is unoccupied in the case of h-WO_3. For all this, the vacant nodes arrange in a strictly ordered way. Such a comparison of the structures of h-WO_3 and UO_3, as well as the similarity of the X-ray diffraction data for UO_3 and h-$WO_{2.8}$, allows us to suppose that the arrangement of the metal atoms in the h-$WO_{2.8}$ phase is intermediate between those of h-WO_3 and UO_3 (see Figure 4b). This supposition allows us to propose a scheme of transformation of the structure when going from h-WO_3 to h-$WO_{2.8}$. During the partial reduction of h-WO_3, vacancies are created on the oxygen sublattice. At a certain quantity of these vacancies, the initial structure of h-WO_3 becomes unstable. Therefore, the structure of h-WO_3 undergoes compression and the anion sublattice rebuilds. In this case, changes observed on the cation sublattice are smaller than those observed on the anion sublattice: the hexagonal motif remains constant and only the partial unordered filling of nodes,

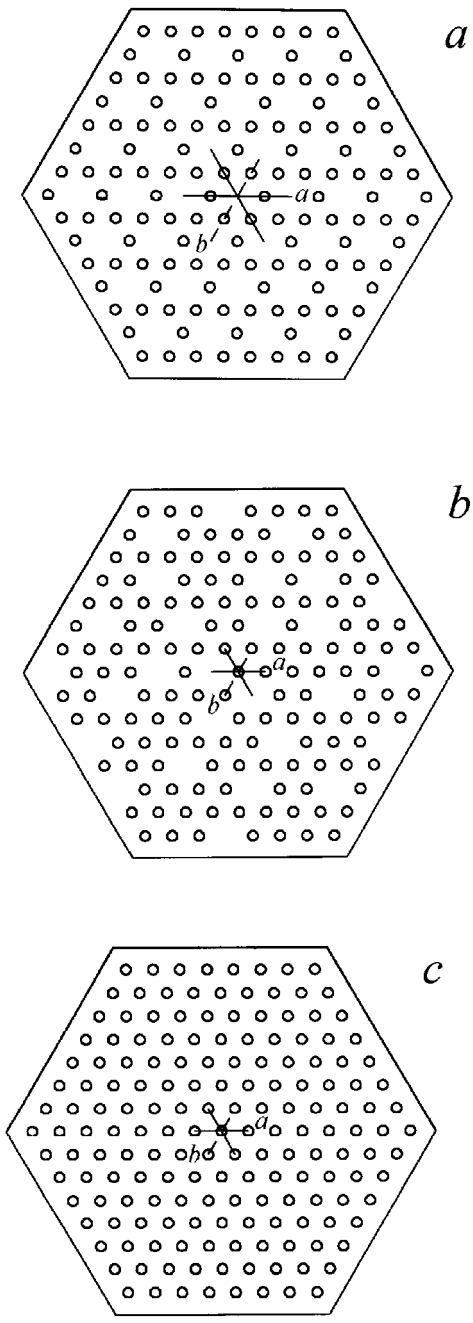

Figure 4. Arrangement of the metal atoms in the (001) plane of (a) h-WO_3, (b) h-$WO_{2.8}$, and (c) UO_3.

which are unoccupied in the structure of h-WO_3, is observed. As a result, the cation sublattice of h-$WO_{2.8}$ represents a hexagonal net, similar to that of UO_3, with an unordered distribution of vacancies. Therefore, it can be assumed that the h-WO_3 → h-$WO_{2.8}$ transition results in partial compression of the structure and leads to transformation of the anion sublattice with appearance of hexagonal close-packed layers created by the oxygen atoms and to disordering the cation sublattice with preservation of its hexagonal motif.

Taking into account the above facts, we can describe the nonstoichiometric $WO_{2.8}$ phase within a model based on a structure of the UO_3 type with disordered arrangement of a certain amount of vacancies on both sublattices. Using the above model, we have carried out an analysis of the X-ray diffraction data within the Rietveld

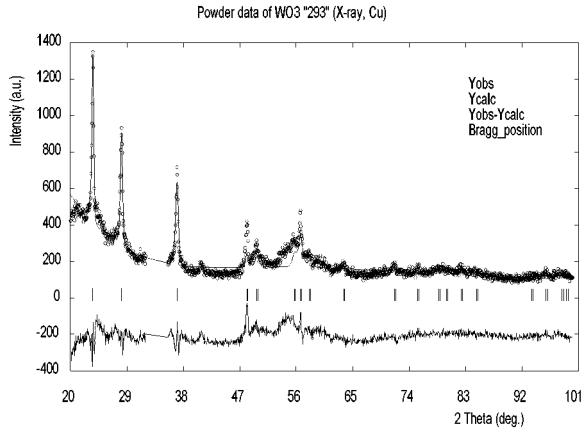

Figure 5. Experimental X-ray powder diffraction data for h-$WO_{2.8}$ (top trace, open circles) and calculated data for this compound using the Rietveld's refinement (top trace, solid line); Bragg's positions (middle trace); difference curve of the experimental and calculated results (bottom trace).

Full Profile Matching & Integrated Intensities Refinement of X-ray and/or Neutron Data Programs, as mentioned in the Experimental Section. Figure 5 represents the results of this analysis. In the present work, the following Rietveld refinement parameters were used: background coefficients; scale; *u*, *v*, and *w* coefficients; preferred orientation; asymmetry parameters; cos θ and sin θ. Fixed parameters were as follows: N_{at}; space group; atom type; cell parameters (*a*, *b*, *c*, α, β, γ); wavelengths. The values of the important parameters were found to be $R_{wp} = 35.3$, $R_f = 29.9$, and $R_e = 25.09$. Taking into account certain textures of the powdered sample and small impurities of the monoclinic $WO_{2.9}$ phase not considered in the present Rietveld refinement as mentioned in the beginning of this section, we observe a rather good coincidence of the experimental and calculated profiles. The results of the above analysis indicate that the lattice parameters of the new hexagonal nonstoichiometric phase, h-$WO_{2.8}$, are as follows: $a = 0.3625$ nm and $c = 0.3780$ nm.

3.2. Electronic Structure. As is known (see, for example, refs 19 and 20), in tungsten oxides the X-ray Mg (or Al) $K\alpha_{3,4}$ satellite excitation of W $4f_{7/2,5/2}$ electrons overlaps the structure of the XPS valence-band spectra owing to photoemission from the O 2s-like states located in the energy region near 22.5 eV binding energies (BEs) with respect to the Fermi energy, E_F. The subtraction of the W $4f_{7/2,5/2}$ core-level spectra, excited by the radiation of the Mg(Al) Kα satellites, from the XPS spectra is a rather difficult problem.[19,20] Therefore, as in refs 10 and 12, in the present work the XPS spectra of h-WO_3 and the nonstoichiometric hexagonal tungsten oxide, h-$WO_{2.8}$, were recorded within a continuous energy range up to 46 eV with respect to E_F, and then the Mg Kα satellite excitations of the W $4f_{7/2,5/2}$ core-level spectra were subtracted using the method successfully applied earlier for XPS studies of substoichiometric tantalum carbides.[21,22] This gives the possibility of obtaining the XPS valence-band spectra, including photoemission from the O 2s-like states. As an example, Figure 6 shows the XPS spectra of the studied compound without any corrections (solid curve 1) and after the subtraction (dashed curve 2) of the XPS W 4f core-level spectra excited by the radiation of the Mg Kα' α_{3-6} satellites. The spectra have been normalized to one and the same integral intensity of the XPS W $4f_{7/2,5/2}$ core-level spectra of the corresponding compound. The results of such normalization indicate that the peak intensity of the XPS valence-band spectra decreases somewhat when going from h-WO_3 to h-$WO_{2.8}$. The relative intensities of the O 2s-like subband (with respect to the intensity of the XPS valence-band spectrum of the corresponding compound) decreases in the sequence h-WO_3 → h-$WO_{2.8}$. This can be explained by the decrease of the oxygen content in the mentioned sequence of compounds. The broad structures representing the XPS O 2s-like subband do not allow us to detect any tendency of a shift of the subband maximum when going from h-WO_3 to h-$WO_{2.8}$. Therefore, as can be seen from Table 2, BEs of the subband maxima remain constant (within experimental error).

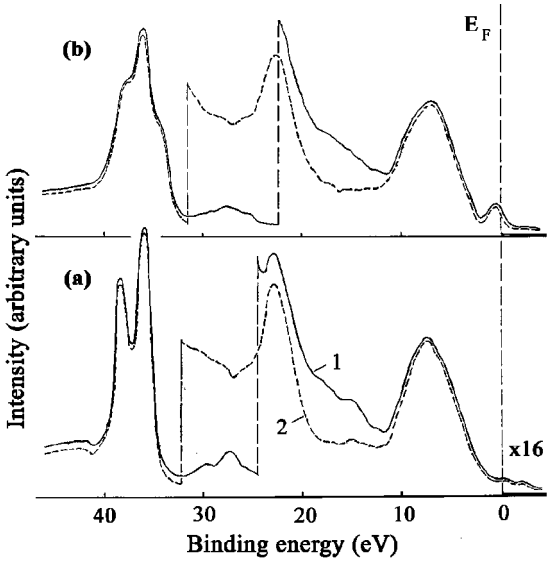

Figure 6. XPS spectra of (a) h-WO_3 and (b) h-$WO_{2.8}$: (1) without any correction; (2) after the subtraction of the W 4f spectra excited by the radiation of the Mg Kα' α_{3-6} satellites.

Table 2. Some Characteristics (in eV) of the XPS Spectra for the Compounds Studied

	BE (half-width)[a]			
compd	XPS O 1s core-level spectrum	XPS W 4f core-level spectrum	max of the XPS O 2s-like subband	half-width of the XPS valence-band spectrum
h-WO_3	530.86 (1.83)	36.02 (3.66)	22.6	6.03
h-$WO_{2.8}$	530.91 (2.05)	35.90 (4.92)	22.5	6.27
uncertainty	±0.05 (±0.08)	±0.05 (±0.05)	±0.1	±0.08

[a] Half-widths are given in parentheses.

As shown in Figure 6, the XPS W 4f core-level spectrum of h-$WO_{2.8}$ shows that the surface of this compound is covered by a thin film of WO_3. We could not eliminate this thin layer of tungsten trioxide on the surface of the h-$WO_{2.8}$ compound using cleaning of the surface by a diamond file. A similar situation was observed earlier when studying nonstoichiometric tungsten oxides with the structure belonging to the monoclinic group:[11,12] the three-peak structure of the W 4f spectra is characteristic for the WO_x compounds, where $2 \leq x < 3$. As can be seen from Table 2, the XPS W 4f

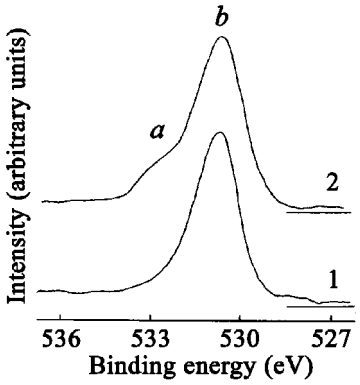

Figure 7. XPS O 1s core-level spectra of (1) h-WO_3 and (2) h-$WO_{2.8}$.

core level spectrum broadens significantly when going from h-WO_3 to h-$WO_{2.8}$.

From Figure 6 one can observe that the XPS valence-band spectra of the nonstoichiometric h-$WO_{2.8}$ compound show the creation of an additional subband at E_F. The subband is absent on the XPS valence-band spectrum of h-WO_3 (as well as of the m-WO_3 compound[10,12]). According to the results of refs 3 and 12, the above near-Fermi subband of the monoclinic $WO_{x<3}$ compounds is created due to the W 5d-like and W 6s-like states taking part in the formation of the shortened W−W bonds in the nonstoichiometric tungsten oxides. It is believed that this is also true for the nonstoichiometric h-$WO_{2.8}$ compound studied. The XPS valence-band half-width increases somewhat in the sequence h-WO_3 → h-$WO_{2.8}$ (Table 2).

As one can see from Figure 7 and Table 2, no changes in the energy positions of the main maxima "b" of the XPS O 1s core-level spectra occur when going from h-WO_3 to h-$WO_{2.8}$. Nevertheless, a small broadening of the XPS O 1s core-level spectra is observed in the above sequence of tungsten oxides (Table 2) due to creation of the feature "a" at ~533 eV BEs on the spectrum of the h-$WO_{2.8}$ compound. According to the results of XPS studies by Kruglov et al.,[23] formation of the above feature on the O 1s spectrum of tungsten oxides is due to crystallized water. Formation of the feature "a" of the spectrum is characteristic for the substoichiometric monoclinic tungsten oxides.[12] As shown in ref 12, the relative intensity of the feature "a" on the XPS O 1s core-level spectrum increased significantly in the sequence $WO_{2.77}$ → WO_2.

4. Conclusion

The nonstoichiometric h-$WO_{2.8}$ phase is synthesized at the initial stage of reduction of hexagonal tungsten trioxide, h-WO_3. The phase keeps the hexagonal structure type of the initial compound. X-ray powder diffraction data and a full-profile analysis using the Rietveld method indicate that the structure of h-$WO_{2.8}$ can be constructed on the basis of the UO_3 structure type with nonordered arrangement of a certain amount of vacancies on the tungsten and oxygen sublattices.

The formation of the early unknown hexagonal $WO_{2.8}$ phase during reduction of h-WO_3 (instead of the monoclinic $WO_{2.9}$ phase which is usually formed during reduction of m-WO_3) indicates that the structure of h-WO_3 is stable, mainly its cation sublattice, during reaction conditions. An analogous phenomenon was already observed by us during selective reduction of copper from $CuWO_4$. In the latter case, the formation of the metastable hexagonal phase h-WO_3 was caused by the stability of the hexagonal motif of the cation sublattice of copper tungstate.

The formation of an additional near-Fermi subband, which is absent in tungsten trioxide, was observed on the XPS valence-band spectrum of the nonstoichiometric hexagonal $WO_{2.8}$ compound. Half-widths of the XPS valence band as well as both W 4f and O 1s core-level spectra increase somewhat in the sequence h-WO_3 → h-$WO_{2.8}$.

References

(1) Magnéli, A. *Ark. Kemi* **1950**, *1*, 513.
(2) Sundberg, M.; Tilley, R. J. D. *J. Solid State Chem.* **1974**, *11*, 150.
(3) de Angelis, B. A.; Schiavello, M. *J. Solid State Chem.* **1977**, *21*, 67.
(4) Iguchi, E.; Salje, E.; Tilley, R. J. D. *J. Solid State Chem.* **1981**, *38*, 342.
(5) Goldschmidt, H. J. *Interstitial Alloys*; Butterworths: London, 1967.
(6) Gerand, B.; Nowogrocki, G.; Guenot, J.; Figlarz, M. *J. Solid State Chem.* **1979**, *29*, 429.
(7) Han, W.; Hibino, M.; Kudo, T. *Bull. Chem. Soc. Jpn.* **1998**, *71*, 933.
(8) Solonin, Yu. M.; Privalov, Yu. G. *Dokl. AN UkrSSR, Ser. B, No. 1* **1985**, 46 (in Russian).
(9) Khyzhun, O. Yu.; Solonin, Yu. M. *Poroshkovaya Metallurgia, No. 5/6* **2000**, 82 (in Russian).
(10) Khyzhun, O. Yu.; Solonin, Yu. M.; Dobrovolsky, V. D. *J. Alloys Compd.* **2001**, *320*, 1.
(11) Khyzhun, O. Yu. *Metallofiz. Noveishie Tekhnol.* **2000**, *22*(3), 55 (in Russian).
(12) Khyzhun, O. Yu. *J. Alloys Compd.* **2000**, *305*, 1.
(13) Hjelm, A.; Granqvist, C. G.; Wills, J. M. *Phys. Rev. B* **1996**, *54*, 2436.
(14) Šušić, M. V.; Solonin, Yu. M. *J. Mater. Sci.* **1988**, *23*, 267.
(15) Khyzhun, O. Yu.; Solonin, Yu. M. *Rep. NASU*, **2000**, *No. 7*, 82.
(16) Solonin, Yu. M. D.Sc. Thesis, Institute for Problems of Materials Science, National Academy of Sciences of Ukraine, Kiev, 1990.
(17) Schafer, H.; Gruehn, R.; Schults, F. *Angew. Chem.* **1966**, *78*, 28.
(18) Shubert, K. *The Crystal Structures of Two-Component Phases*; Metallurgiya: Moscow, 1971 (in Russian).
(19) Siegbahn, K.; Nordling, C.; Fahlman, A.; Nordberg, R.; Hamrin, K.; Hedman, J.; Johansson, G.; Bergmark, T.; Karlsson, S.-E.; Lindberg, I.; Lindberg, B. *ESCA-Atomic, Molecular and Solid-State Structure Studied by Means of Electron Spectroscopy*; Almqvist and Wiksells: Stockholm, Sweden, 1967.
(20) Nefedov, V. I. *Handbook on X-ray Photoelectron Spectroscopy of Chemical Compounds*, Khimia: Moscow, 1984 (in Russian).
(21) Khyzhun, O. Yu.; Zhurakovsky, E. A.; Sinelnichenko, A. K.; Kolyagin, V. A. *J. Electron Spectrosc. Relat. Phenom.* **1996**, *82*, 179.
(22) Khyzhun, O. Yu. *J. Alloys Compd.* **1997**, *259*, 47.
(23) Kruglov, V. I.; Denisov, E. P.; Kraevski, S. L. In *Oxide Electrochromic Materials*; Lusis, A., Ed.; Latvian State University: Riga, Latvia, 1981; p 66.

CG015545Z